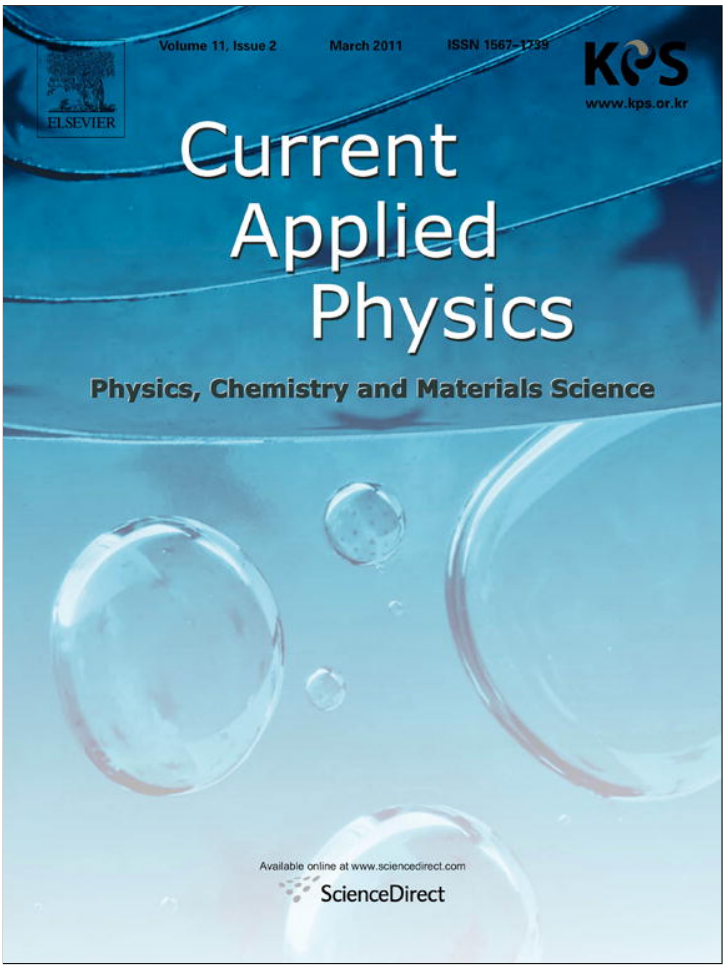

Current Applied Physics 10 (2010) e113–e117

Contents lists available at ScienceDirect

Current Applied Physics

journal homepage: www.elsevier.com/locate/cap

Effects of stabilization temperatures on electro-optic characteristics of polymer-stabilized optically isotropic liquid crystals

Miyoung Kim [a,b], Byeong Gyun Kang [c], Min Su Kim [b], Mi-Kyung Kim [b], Myong-Hoon Lee [b], Shin-Woong Kang [c,**], Seung Hee Lee [b,c,*]

[a] Korea electronics technology institute Palbokdong 2-ga, Deokjin-gu, Jeonju, Jeonbuk 561-844, Republic of Korea
[b] Polymer Fusion Research Center, Department of Polymer-Nano Science and Technology, Chonbuk National University, 1Ga 664-14, Deokjin-dong, Deokjin-ku, Jeonju, Chonbuk 561-756, Republic of Korea
[c] Department of BIN Fusion Technology, Chonbuk National University, Jeonju, Jeonbuk 561-756, Republic of Korea

ARTICLE INFO

Article history:
Received 3 January 2010
Received in revised form
28 April 2010
Accepted 10 June 2010
Available online 30 June 2010

Keywords:
Liquid crystals
Blue phases
Kerr effect
Stabilization temperature

ABSTRACT

Polymer stabilization of a single cholesteric LC mixture with a short pitch has been performed at different temperatures near the transition from nematic to isotropic phases. Depending on the stabilization temperatures, the LC/polymer composites under applied electric field exhibit significantly different electro-optic properties. Although, in all cases, optical birefringence is induced by the *Kerr effect* from initially optically isotropic LC states, phase structures, morphology of the stabilizing polymer networks, and electro-optic properties such as contrast ratio, hysteresis and threshold voltage of the cells, crucially rely on the stabilization temperatures. Based on the polymer morphology and electro-optic characteristics, we conjecture that the stabilization temperature affects the nanoscopic structure of LC phase *prior to* and consequently *after* the polymer stabilization.

1. Introduction

Currently commercial liquid crystal displays utilize the nematic LCs with various operating modes such as twisted nematic (TN), in-plane switching (IPS) [1], fringe-field switching (FFS) [2,3] and multi-domain vertical alignment (MVA) [4]. Although they have been achieved a great deal of improvements on display qualities, still challenging demands exist in the field such as, especially, fast response time, high contrast ratio, wide viewing-angle, low cost, and low energy consumption.

Very recently, blue phase and nanostructured LCs of short pitch cholesteric liquid crystals have attracted great attentions due to their promising properties for display applications [5–7]. Superiority of these modes mainly stems from their optical isotropy, originated from nanoscopic organizations of cholesteric LCs. For both cases, optical isotropy makes an ideal dark state even without use of optical compensation films and thus realize high contrast ratio of devices. In addition, no surface treatment for LC alignment is necessary so that the simpler process can reduce a production cost, and sub-millisecond response time facilitates fast moving pictures of displays [8–12]. Polymer stabilization was previously proposed, for practical applications, to solve the hurdles such as a temperature range of a panel operation for the cholesteric blue phase and induce an optically isotropic nanostructured cholesteric LC phase [8,9,12,13].

In these optically isotropic LC states, a field-off state under crossed polarizers is completely dark (i.e., ideal off-state) according to nanoscopic organizations. In the presence of an electric field, optical birefringence of LC is induced in a practical range of applied voltage due to its intrinsic liquid crystalline order and its magnitude is determined by,

$$\Delta n_i = \lambda K E^2$$

where Δn_i is the induced birefringence, λ is the wavelength of an incident light, K is the *Kerr constant* of the LC mixture and E is an electric field [9]. The normalized transmittance of the device associated with a phase retardation can be described as follows:

$$T/T_0 = \sin^2 2\psi(V) \sin^2(\pi d \Delta n_i(V)/\lambda)$$

Where $\psi(V)$ is a voltage dependant angle between one of the transmission axes of the crossed polarizers and the LC director, d is

* Corresponding author. Polymer Fusion Research Center, Department of Polymer-Nano Science and Engineering, 1Ga 664-14, Deokjin-dong, Deokjin-ku, Jeonju, Chonbuk 561-756 , Republic of Korea. Tel.: +82 63 270 2343; fax: +82 63 270 2341.
** Corresponding author. Tel.: +82 63 270 2343; fax: +82 63 270 2341.
E-mail addresses: swkang@jbnu.ac.kr (S.H. Kang), lsh1@chonbuk.ac.kr (S.H. Lee).

1567-1739/$ – see front matter © 2010 Elsevier B.V. All rights reserved.
doi:10.1016/j.cap.2010.06.011

thickness of LC layer with induced birefringence, and Δn_i (V) is induced birefringence as function of applied voltage. In order to maximize the transmittance, ψ should be equal to 45° and $d\Delta n_i$ should be $\lambda/2$ [14].

In this report, we have studied the effects of a stabilization temperature on electro-optic properties and network morphologies of the polymer-stabilized short pitch cholesteric LCs. For the study, a single cholesteric mixture with the blue phase was stabilized by photo-polymerization of reactive mesogens in the mixture at different temperatures near the blue phase–isotropic transition. The electro-optic characteristics and network morphologies formed at different temperatures imply that the blue phase breaks up into domains smaller than wavelengths of visible light while temperature is approaching to the isotropic transition from the blue phase.

2. Experiments

2.1. Preparation of electro-optic cells

For the experiments, electro-optic cells with interdigitated electrodes were fabricated [15]. The bottom substrate consisted of pixel electrodes with patterned indium-tin-oxide (ITO) and common electrodes with patterned Mo–Ti alloy on a flat glass. The width and separation of patterned-electrodes with a wedge shape were 4 μm and 6 μm, respectively [15]. Plastic balls with 6 μm diameter were used to maintain the gap between top and bottom substrates. The measured gap of empty cells prior to LC load was 6.0 ± 0.1 μm. The dimension of cells used for experiments were 3 cm × 3.2 cm with an active area of 2 cm × 2 cm.

2.2. Preparation of LC mixture

Our sample was a mixture of the nematic liquid crystal, chiral dopants, reactive monomers, and a photoinitiator (Irgacure 651, Ciba Additive Corp.) The nematic LC used was a cyano-biphenyl type mixture purchased from Merck. We used two reactive monomers, nonmesogenic Ethylhexyl acrylate EHA (Aldrich) and the nematic mesogen RM 257 (Merck). The chiral dopants were ZLI 4572 and CB-15 both from Merck. The sample components were mixed in the following weight ratio: nematic LC (33.0), chiral dopants (18.5), RM 257 and EHA (47.9), and photoinitiator (0.6).

2.3. Polymer stabilization

The mixture was then filled into 6 μm-thick electro-optic cells described above at isotropic temperature (100 °C). The samples were cooled to stabilization temperatures and annealed at least for 5 min before the exposure with UV-light which initiate photo-polymerization of reactive monomers. The samples were exposed with UV-light generated by an Hg–Xe source L9588-01 (Hamamatsu) for 2 h with an intensity of 5 mW/cm^2. The exposure conditions were the same for three samples except for the stabilization temperatures.

2.4. Polarizing optical microscopy

The cells loaded with a cholesteric mixture were placed under Nikon DXM1200 polarizing optical microscope with crossed polarizers in a transmission mode. The optical textures and electro-optic switching behaviors were examined before and after polymer stabilization at different temperatures. The microphotographic images were recorded using a Nikon digital camera DXM1200.

2.5. Electro-optical measurements

The electro-optical textures of the test cells were observed by the optical polarizing microscope (Nikon DXM1200) by applying

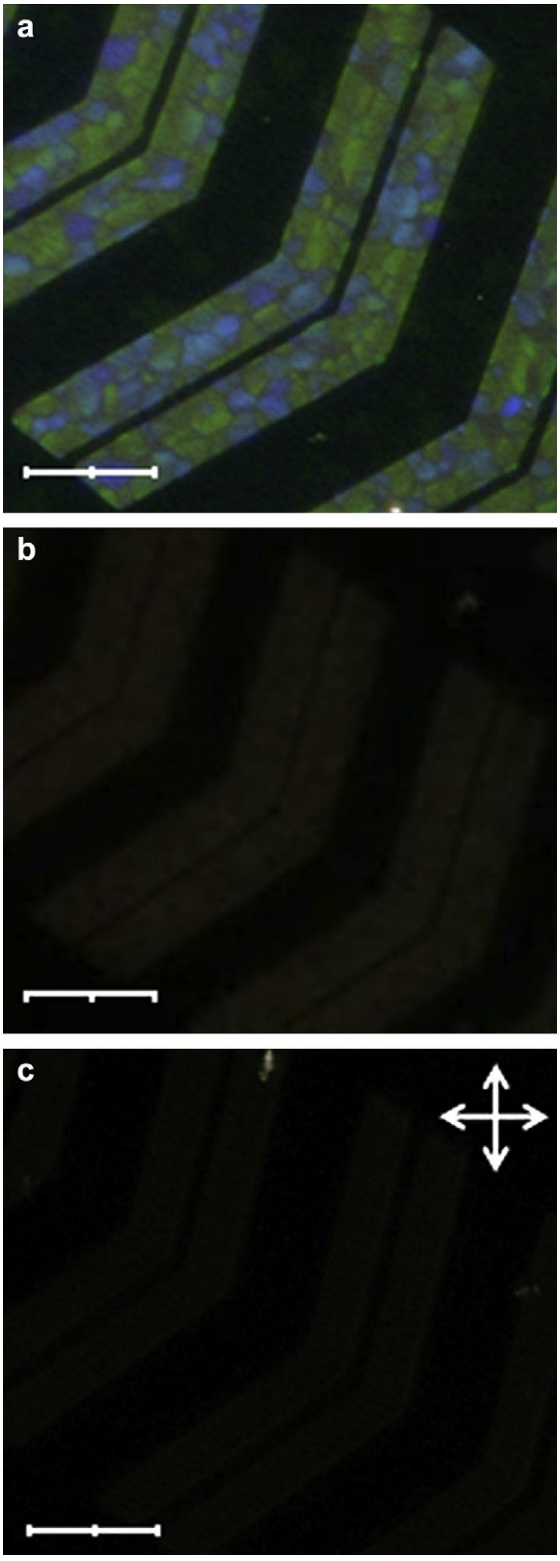

Fig. 1. Polarizing optical micrographs of the LC mixture confined in a Super IPS cell prior to the polymer stabilization: at (a) T_{BP}, (b) T_{OILC1}, and (c) T_{OILC2}. The inset arrows represent polarizer directions. The scale bars correspond to 50 μm.

square waveform electric field at 60 Hz. The optical transmittance was calculated using an image analyzer i-solution (*i*MTechnoloy).

2.6. Scanning electron Microscopy

For the SEM experiment, cells were fabricated using bare glasses as substrates to avoid nonuniform exposure of UV-light across the sample. The samples with bare polymer networks were prepared by selectively dissolving LCs in hexane. After removal of LCs and solvent, a thin gold layer was deposited. The polymer network morphology was then observed using a field emission scanning electron microscope (S-4300SE, Hitachi) operated at 10 kV in secondary electron imaging mode.

3. Results and discussion

The cholesteric mixture used in our experiments exhibits the cholesteric phase up to 90.0 °C. The blue phase (BP) with a platelet texture appears at the temperature ranging from 90.0 °C to 92.0 °C. On further heating, the sample turns into dark grayish state under crossed polarizers. The mixture reaches to a complete isotropic phase at 95.0 °C. The mixture confined in standard cells at room temperature displays a typical *Grandjean texture*, where the cholesteric helical axis is aligned normal to the substrates with some disclination lines. In the blue phase, characteristic platelet textures were observed. The size of platelets with a blue or yellowish green color ranges about 10–30 μm. As temperature approaches to the isotropic transition, the optical image turns into more grayish and darker state as seen in Fig. 1a displays a typical platelet texture of the blue phase confined in the cell at 90.2 °C. Fig. 1b (93.8 °C) and 1c (100 °C) show a decrease in optical transmission, indicating a transformation to a more optically isotropic structure. It is important to note that the optical images were obtained at the elevated backlight intensity and a sensitivity of the digital camera in the latter two cases. Since structures of these states are unclear at this stage, we label each phase *OILC1* and *OILC2* with corresponding temperatures T_{OILC1} and T_{OILC2}, respectively. It should be emphasized that this state is crucially different from the isotropic phase although it appears to be a transition to isotropic phase. Due to the small *Kerr effect* of the isotropic phase, no noticeable optical birefringence was observed by applying electric field up to breakdown voltage. However, for the *OILC1* and *OILC2*, relatively small electric field could induce large optical birefringence. This strongly indicates that the local molecular ordering in the *OILC1* and *OILC2* states is mesomorphic and thus results in a much larger *Kerr constant* compared to the isotropic phase.

Fig. 2a–c show polarizing optical micrographs of the samples after polymer stabilization facilitated by photo-induced polymerization of reactive monomers in the LC mixture. In Fig. 2a, stabilized at the temperature (T_{BP} = 90.2 °C) of a blue phase, the platelet boundaries are less noticeable and colors due to a selective reflection of the BP shifted towards a blue. This implies that a pitch of the cholesteric LC becomes shorter after the reactive monomers are phase separated and forms polymer networks that stabilize the BP phase of a host LC mixture. However, no clear difference in the POM images was observed during stabilization of *OILC1* and *OILC2* states as shown in Fig. 2b and c. For all cases, the cholesteric Grandjean texture was not observed at room temperature. This ensures that all three different states were stabilized and retained their microscopic organizations by the internal polymer networks. It is obvious that the composition of a liquid crystalline cholesteric mixture was significantly altered by the phase separation of reactive mesogens into polymerized solid networks. As a result, the phase transition temperature from liquid crystal to isotropic liquid phase is also significantly shifted to 70.0 °C after the polymer stabilization (i.e., 25 °C difference between before and after polymerization). This was confirmed by the field-induced birefringence as a function of temperature. However, no measurable difference in the transition temperature was observed among three samples stabilized at different temperatures.

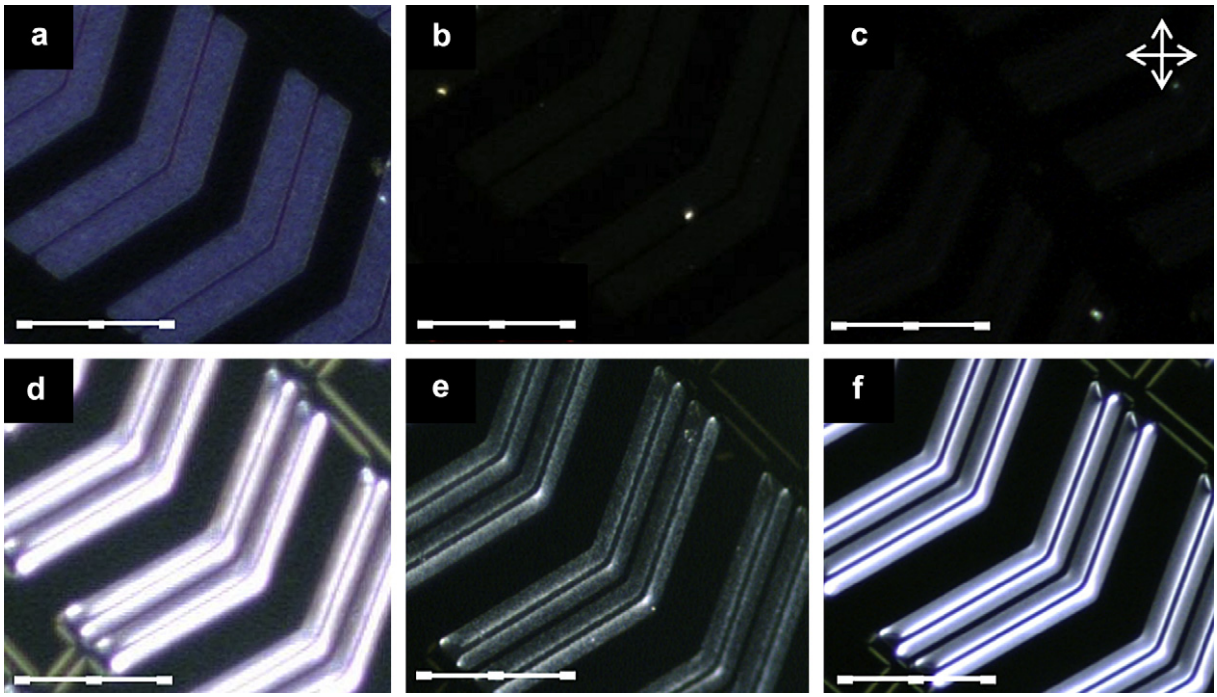

Fig. 2. Polarizing optical microphotograghs of the polymer-stabilized LCs in a Super IPS cell without (a–c) and with (d–f) 6 V/μm of applied electric field at room temperature: Stabilized at (a, d) T_{BP}, (b, e) T_{OILC1}, and (c, f) T_{OILC2}. The inset arrows represent polarizer directions and can be applied for all images. The scale bars correspond to 100 μm.

For the samples obtained at the T_{BP} and T_{OILC2}, a significant amount of birefringence was induced by applying about 6 V/μm and continuously increases with field strength. For the sample formed at the T_{OILC1}, however, the threshold field for an induced optical birefringence was much higher and the bright-state of the cell was limited compared to other samples as shown in Fig. 2d–f. It is uncertain what is responsible for this result. By taking the dark state (i.e., off-state) into consideration, the cell stabilized at the T_{OILC2} exhibits the best contrast ratio.

Fig. 3 demonstrates an electro-optic hysteresis of the polymer-stabilized LC composites. All three samples exhibit a large hysteretic response upon applied electric field. It is unclear what is responsible for the hysteresis. Compared to the previous reports [16–18], however, relatively large amount of reactive mesogen that was a component of the LC mixture is separated during polymerization reaction and becomes solid networks. Consequently, the cholesteric pitch may be continuously altered by the progress of polymerization. Presumably this is one potential source of a large hysteresis compared to previous polymer-stabilized blue phase [16]. Although a large portion of reactive monomer is beneficial for the stabilization, another disadvantage of the system is more portions of the composite sample that are not responsive to an electric field. This may result in a low induced optical birefringence and thus limit the maximum transmittance of a device. It should also be noted that, at zero field, the original optical state (i.e., dark state prior to applying electric field) is not completely restored after applying electric field as seen in Fig. 3. To recondition the primitive stabilized state, sample should be heated to the temperature employed for stabilization.

To investigate network morphology, we performed real-space imaging of the bare network using a scanning electron microscope. The representative SEM data obtained on multiple samples are presented in Fig. 4a displays the network morphology formed in the blue phase (i.e., polymerized at T_{BP}). The bead-like polymer aggregates are fused into clusters and they form a global structure with regularly arranged empty tunnels that were occupied by LC mixture. The LC tunnels are observed in all three primary directions of the sample and the diameter of holes is approximately 800 nm. On the other hand, the networks formed at the T_{OILC1} shown in Fig. 4b exhibit features of more solid lumps. The LC channels (i.e., empty space in SEM image) are not vey well defined and the regularity breaks in short distance range compared to that from the blue phase. In case of the network obtained at the T_{OILC2}, the local morphology is similar to that from the blue phase. However, the structure of a global network is significantly different. The clusters of polymer aggregates are randomly oriented in this case and no regular LC tunnels are observed. This may indicate that the structure of blue phase is completely disappeared due to either stabilization temperature or phase separation of reactive mesogen RM 257 from the LC mixture. The optical isotropy may be attributed to the random nanoscopic structure of small domains with a nematic LC order for both before and after stabilization.

It is well documented that the reactive mesogens polymerized in the LC media can be phase separated into specific areas, and thus

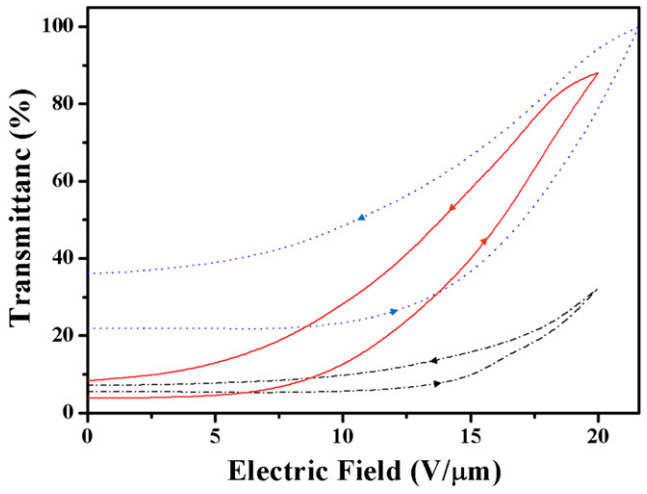

Fig. 3. Electro-optic hysteresis of the polymer-stabilized LCs formed at T_{BP} (blue dotted line), T_{OILC1} (black broken line), and T_{OILC2} (red solid line). The arrows represent increase and decrease of an applied electric field.

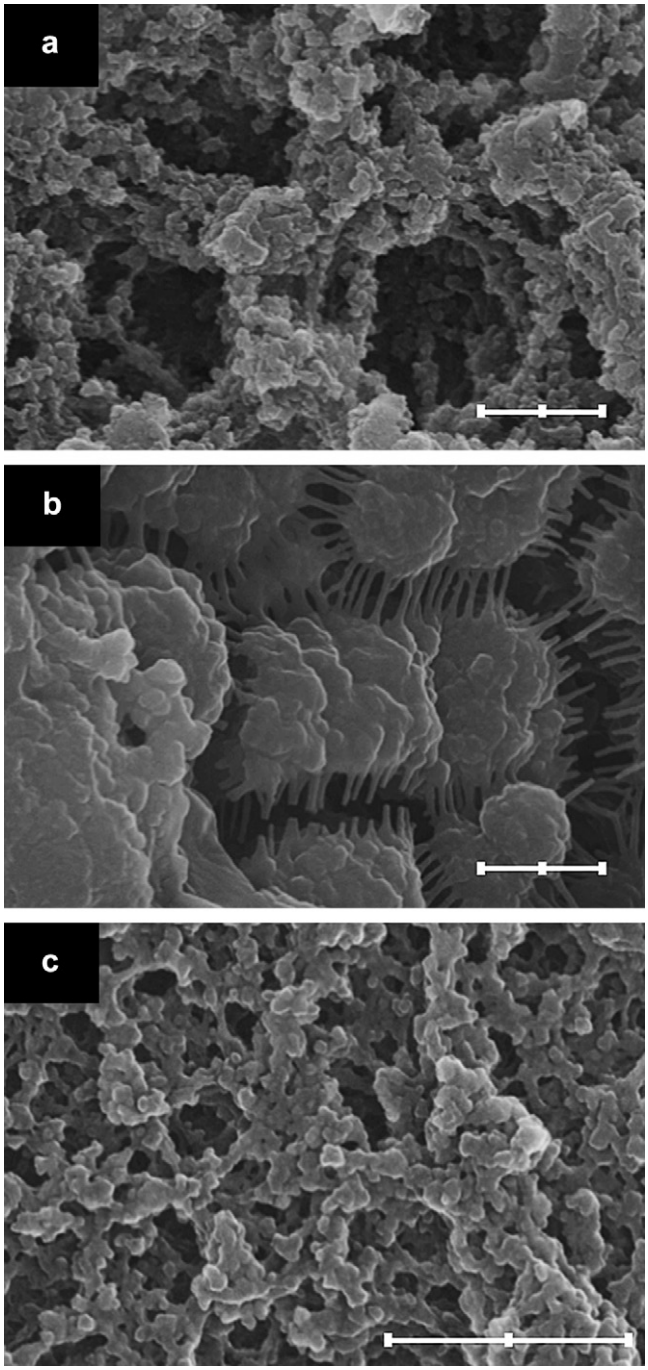

Fig. 4. The SEM micrographs of polymer networks formed at (a) T_{BP}, (b) T_{OILC1} (c) T_{OILC2}. All images were taken from the normal view to the substrate. The scale bars represent 500 nm. The distinct network morphologies represent a crucial difference for the structures of a host LC.

form patterned networks [19–22]. Since the network structure reflects orientational and spatial order of host LCs, it is useful to conjecture the director configuration of host liquid crystals. In this regard, our SEM observation strongly suggests that the *BP*, *OILC1* and *OILC2* phases bear different macroscopic structures at the conditions prior to polymer stabilization. Therefore they result in morphological difference of the networks. This conclusion is also supported by the distinct optical and electro-optical characteristics of the phases before and after polymerization. Although all phases have locally nematic order, their global organizations are dissimilar each other and hence show distinct E.O. behaviors. It should be noted that the cholesteric pitch of LC mixture can continuously be changed during polymerization because the large amount of RM 257 are polymerized and phase separated from the mixture. This may alter the physical properties, phase transition, and thus structure of LC phases.

4. Conclusions

The polymer-stabilized optically isotropic phases of short pitch cholesterics, obtained at different temperatures near the BP to isotropic transition, exhibit distinct optical, electro-optical and morphological characteristics. The long range structure of a blue phase in a platelet texture breaks up into smaller domains by the increase of temperature before the mixture reaches to the isotropic phase. The LC mixture forms random nanostructure while maintaining nematic LC order near the nematic to isotropic transition. These can be successfully stabilized using photo-polymerization of reactive mesogens and consequently a temperature range for the optically isotropic phases is dramatically expanded to a room temperature.

Acknowledgement

This work was supported by WCU program through MEST (R31-2008-000-20029-0).

References

[1] M. Oh-E, K. Kondo, Appl. Phys. Lett. 67 (1995) 3895.
[2] S.H. Lee, S.L. Lee, H.Y. Kim, Appl. Phys. Lett. 73 (1998) 2881.
[3] J.W. Park, Y.J. Ahn, J.H. Jung, S.H. Lee, Appl. Phys. Lett. 93 (2008) 081103.
[4] A. Takeda, S. Kataoka, T. Sasaki, H. Chida, H. Tsuda, K. Ohmuro, T. Sasabayashi, Y. Koike, K. Okamoto, SID Int. Symp. Dig. Tech. Pap. 29 (1998) 1077.
[5] K. Higashiguchi, K. Yasui, H. Kikuchi, J. Am. Chem. Soc. 130 (2008) 6327.
[6] W. He, G. Pan, Z. Yang, D. Zhao, G. Niu, W. Huang, X. Yuan, J. Guo, H. Cao, H. Yang, Adv. Mater. 21 (2009) 2050.
[7] Y. Tanabe, H. Furue, J. Hatano, Mater. Sci. Eng. B. 120 (2005) 41.
[8] H. Kikuchi, M. Yokota, Y. Hisakado, H. Yang, T. Kajiyama, Nat. Mater. 1 (2002) 64.
[9] Y. Hisakado, H. Kikuchi, T. Nagamura, T. Kajiyama, Adv. Mater. 17 (2005) 96.
[10] Y. Haseba, H. Kikuchi, J. Soc. Inf. Disp. 14 (2006) 551.
[11] H. Kikuchi, H. Higuchi, Y. Haseba, T. Iwata, SID Int. Symp. Dig. Tech. Pap. 38 (2007) 1737.
[12] S.W. Choi, S. Yamamoto, Y. Haseba, H. Higuchi, H. Kikuchi, Appl. Phys. Lett. 92 (2008) 043119.
[13] Z. Ge, S. Gauza, M. Jiao, H. Xianyu, S.-T. Wu, Appl. Phys. Lett. 94 (2009) 101104.
[14] M. Kim, M.S. Kim, B.G. Kang, M.-K. Kim, S. Yoon, S.H. Lee, Z. Ge, L. Rao, S. Gauza, S.-T. Wu, J. Phys. D Appl. Phys. 42 (2009) 235502.
[15] H.H.H. Klausmann, S. Aratani, K. Kondo, J. Appl. Phys. 83 (1998) 15.
[16] Y.-C. Yang, R. Bao, K. Li, D.-K. Yang, SID Int. Symp. Dig. Tech. Pap. 40 (2009) 478.
[17] H. Kikuchi, Y. Haseba, S. Yamamoto, T. Iwata, H. Higuchi, SID Int. Symp. Dig. Tech. Pap. 40 (2009) 578.
[18] L. Lu, J.-Y. Hwang, L.-C. Chien, SID Int. Symp. Dig. Tech. Pap. 40 (2009) 1608.
[19] S.W. Kang, S. Sprunt, L.C. Chien, Appl. Phys. Lett. 76 (2000) 3516.
[20] S.W. Kang, S. Sprunt, L.-C. Chien, Adv. Mater. 13 (2001) 1179.
[21] S.W. Kang, S. Sprunt, L.C. Chien, Macromolecules 35 (2002) 9372.
[22] S.W. Kang, S.H. Jin, L.-C. Chien, S. Sprunt, Adv. Funct. Mater. 14 (2004) 329.